X-RAY FLUORESCENCE PARTICLE SIZE AND SCATTERING ANGLE CONSIDERATIONS– PREPARATORY EXPERIMENTS FOR THE CALIBRATION AND INTERPRETATION OF C1XS DATA

S. Z. Weider[1,2], J. Gow[3], K. H. Joy[1,2,4], I. A. Crawford[1], D. R. Smith[3], A. D. Holland[3], B. M. Swinyard[2], [1]The Joint UCL/Birkbeck Research School of Earth Sciences, Gower Street, London, WC1E 6BT, UK, [2]The Rutherford Appleton Laboratory, Chilton, Oxfordshire, OX11 0QX, UK, [3]e2v centre for electronic imaging, School of Engineering and Design, Brunel University, Uxbridge, Middlesex, UB8 3PH, UK, [4]IARC, Dept. of Mineralogy, The Natural History Museum London, Cromwell Road, London, SW7 5BD, UK. (s.weider@ucl.ac.uk).

Introduction: ISRO's Chandrayaan-1 mission to the Moon is due to be launched in April 2008. Part of its payload is C1XS, a compact X-ray fluorescence (XRF) spectrometer which will provide high quality elemental mapping of the lunar surface [1]. In flight, the input source (solar X-ray spectrum) will be measured by the accompanying XSM payload [2]. An 'in-house' IDL XRF modelling code (referred to as the 'C1XS XRF code' [3]), which is based on the methods of [4], will be used to convert the C1XS data from X-ray fluxes into elemental ratios and abundances. This study outlines a plan of testing the accuracy and robustness of the code, using XRF spectral data from well characterised geological samples. We aim to quantify how XRF intensity varies with changing particle size and phase angle (θ in Fig. 1) geometry, in order to simulate changes in the solar aspect angle (angle between the Sun, the lunar surface and the detectors), as well as surface topography. These issues have previously been studied within a materials science context e.g. [5 – 9], but rarely for heterogeneous, geological samples [10 – 12].

XRF Technique Background: Planetary XRF observations are limited to inner solar system bodies such as the Moon, Mercury and asteroids which have no atmospheres to absorb the low-energy incident and fluorescent X-rays, and where the solar flux is sufficient to create a detectable XRF response [13]. Incident solar X-rays only penetrate into the very top of planetary surfaces (the top 100 μm); hence fluorescent X-rays are produced from very shallow depths [4, 13, 14]. On bodies with regoliths, such as the Moon, it is therefore assumed that the composition of the upper regolith is representative of the underlying bed rock.

The lunar surface is not flat and homogeneous; its diverse grain size population, topography and local chemical variations add complexity to the analysis of remotely sensed XRF data [4]. To a certain extent, in the actual lunar data, the effects of these fluctuations will be reduced by the averaging effect of the wide field of view (25 km FWHM for C1XS), but it is still important to characterise the sensitivity of the modelling software to realistic regolith properties and different illumination conditions. This is the aim of the work here.

Experimental Set-up: The experiments are being carried out at Brunel University, UK, within the e2v centre for electronic imaging (CEI). The equipment is very similar to that used in assessing the effectiveness of the C1XS flight detectors [15].

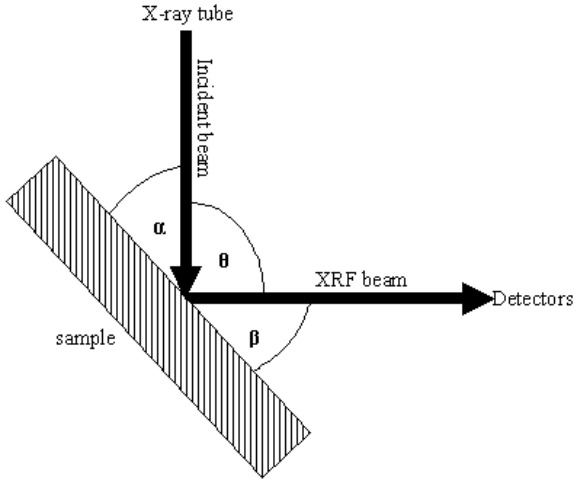

Fig. 1. Simplified geometry of the experimental set-up.

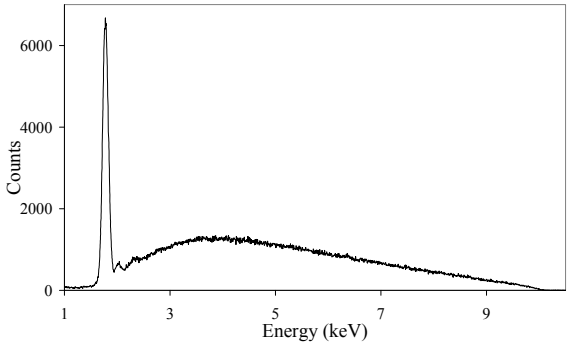

Fig. 2. Measured input beam spectrum, obtained over 30 minutes with a tube potential of 10kV and a current of 0.2mA. This shows a bremsstrahlung curve with a peak at about 1.8 keV, corresponding to the M-series for tungsten (the anode).

A desktop vacuum chamber is attached to an Oxford Instruments X-ray tube with a tungsten source. The X-rays pass through an aluminium tube and are then collimated through a small central hole in a copper plate into the main chamber. Target materials are mounted onto a central Al octagonal

sample holder which can be rotated into the beam's path and used to alter the angle of incidence (and emergence) of the beam onto the sample. The X-ray beam has an effective area of about 2 x 4 mm. A detector module containing four e2v technologies CCD54 swept charge device (SCD) detectors is housed within a camera head attached to the front of the vacuum chamber. The detector array is mounted on a shapal (aluminium nitride ceramic) cold finger attached to a thermo-electric cooler. This arrangement allows the SCDs to be operated at low temperatures (as low as ~ -40ºC). The input beam spectrum has been characterised using a Si-Li detector (Fig. 2).

Sample Material: A number of different rock samples have been acquired for use in this experiment: (1) *anorthosite* – a terrestrial sample, rich in anorthite (plagioclase), which is a good representation of lunar highland material; (2) *icelandite* – basaltic-andesitic in composition, which has a very fine-grained texture; (3) *Etna basalt* – fine-grained crystalline matrix with small (~1 mm) phenocrysts of pyroxene and plagioclase; (4) *peridotite* – mantle xenolith, rich in olivine with accessory spinel and pyroxene, therefore low in SiO_2 and high in MgO and FeO, and; (5) *lunar regolith simulant* (JSC-1A) – powdered basaltic regolith simulant developed by NASA [16]. The rocks have been prepared in a variety of ways, in order, (a) to create samples fit to place in the vacuum chamber and (b) to preserve different characteristics of the samples.

Sample preparation: So far, samples prepared include: (1) flat, polished thick-sections (~1 mm) of anorthosite, icelandite, Etna basalt and peridotite; (2) compressed pellets of JSC-1A (pellets of icelandite, Etna basalt and peridotite may also be made up) and; (3) powders of various grain sizes mounted on glass slides using vacuum-safe polymide glue (e.g. Fig. 3). Powders have been created for all the rocks other than the anorthosite (due to lack of material), and then sieved into four grain-size fractions (250 µm to 500 µm, 125 µm to 250 µm, 75 µm to 125 µm, <75 µm). The lunar regolith has a grain-size population most similar to the smaller grain-size fractions [17]. A glass slide with glued JSC-1A has also been prepared. By comparing the spectra from each of the differently prepared samples from the same rock, the effect of different grain sizes and sample preparations on the resulting spectra will be determined.

Qualification of the XRF Modelling Code: The 'C1XS XRF code' will be tested by inputting our laboratory measured X-ray spectra, the observation viewing geometry, a response matrix of the SCD detectors, and the measured input X-ray spectrum to generate a theoretically modelled best-fit rock composition. This modelled composition can then be compared to the sample's known bulk composition (measured using ICP-MS at the Natural History Museum). This comparison will then enable us to verify the reliability of the C1XS XRF code.

Fig. 3. Glass slide sample of glued peridotite powder from the 250 µm to 500 µm grain-size fraction. Green grains are forsteritic olivine and black grains are spinel mineral phases.

Acknowledgements: Thanks to Orbitec and NASA for providing JSC-1A.

References: [1] Grande, M. et al. (2007) *(ICEUM9/ILC2007),* Abstract #110. [2] Huovelin, J. et al. (2002) *Planetary and Space Science, 50,* 1345-1353. [3] Swinyard, B. M. (1999) *CCLRC Document number: S1-CIX-RAL-TN-3029 Issue/Rev. No: 1.* [4] Clark, P. E. and Trombka, J. I. (1997) *JGR, 102,* 16631-16384. [5] DeWolff, P. M. (1956) *Acta Cryst., 9,* 682-683. [6] Claisse, F. and Samson, C. (1962) *Advances in X-ray Analysis, 5,* 335-354. [7] Paakkari, T. and Suortti, P. (1968) *Acta Cryst., A24,* 701-702. [8] Berry, P. F. et al. (1969) *Advances in X-ray Analysis, 12,* 612-632. [9] Hawthorne, A. R. and Gardner, R. P. (1978) *X-ray Spectrometry, 7,* 198-205. [10] Okada, T. and Kuwada, Y. (1997) *LPS XXVIII,* Abstract #1708. [11] Okada, T. et al. (1998) *LPS XXIX,* Abstract #1597. [12] Maruyama, Y. et al. (2007) *LPS XXXVIII,* Abstract #1186. [13] Yin, L. I. et al. (1993) Remote Geochemical Analysis: Elemental and Mineralogical Composition, *Cambridge University Press, Cambridge*. [14] Adler, I. et al. (1973) *The Moon, 7,* 487-504. [15] Gow, J. et al. (2007) *e2v centre for electronic imaging, Brunel University, Report: Brunel_Chandrayann_TR_005.01.* [16] Carpenter, P. (2006) ***www.lunarmarssimulant.com*** [17] McKay, D. S. et al. (1991). In: Lunar Sourcebook, *Cambridge University Press, Cambridge* p. 285.